

Residual strength assessment for a butt joint in MSD condition

C. Calì, R. Citarella*

Mechanical Engineering Department, Università degli Studi di Salerno, Via Ponte Don Melillo, Fisciano (Salerno), Italy

Abstract

The present work summarises a numerical procedure aimed to the residual strength assessment of a cracked butt joint, based on R-curve analysis and plastic collapse prediction. In a linear elastic fracture analysis, the SIF's (Stress Intensity Factors) evaluation is based on the use of the Dual Boundary Element Method, as implemented in the BEASY code. A two-dimensional approximation (plane stress) of the joint is also validated by a 3D numerical analysis which allow to take into account the secondary bending effect and to assess its relevance. Experimental joint collapse load was available for comparison with numerical results, in order to validate the procedure.

Keywords: Residual strength; Secondary bending; Butt joint; BEM; Plastic collapse

1. Introduction

The failure criteria, concerning the unstable crack growth [1-3] under static load, can be written as:

$$K_I \geq K_{Ic} \quad (\text{plane strain}) \quad \text{or} \quad K_I \geq K_c \quad (\text{plane stress}) \quad (1)$$

where K_{Ic} and K_c are called the *fracture toughness* of the material. It is experimentally proved that K_{Ic} is constant for thick sections of a given material whilst K_c , applicable to thinner sections where stable crack

growth can occur, is found to vary with crack length and component geometry. There are no generally accepted quantitative models for the variation of K_c with thickness; some suggested models have been discussed, among the others by Broek [4]. In order to describe the apparent variation of K_c at both short and long crack lengths, Feddersen has suggested a simple model for use in engineering design [5].

From eqns (1) the failure criterion can be written as (Y is the geometry factor):

$$s_c = \frac{K_c}{Y\sqrt{pa_c}} \quad (2)$$

The critical stress s_c must not be exceeded by the operating stress if static failure of the cracked component is to be avoided. The critical stress will decrease as the crack length becomes longer; this must be considered in the long term assessment of working stresses.

The above criteria does not take into account stable crack growth which can occur in thin sections of some materials. As a matter of fact, the failure criteria for plane strain state cannot be extended to the case of thin metal sheet structures, because of extensive slow stable growth under monotonic loading, prior to instability and catastrophic failure. Under these condition the crack will only grow if the load is increasing; if the load is constant the crack will stop. Here, rather than a single material parameter, a material curve is necessary to make an accurate failure prediction. Such curve is called R-curve or K_R -curve and represents an infinity of potential failure points (the crack length at instability is not known a priori).

An explanation of stable crack growth was formulated, suggesting that the increase in crack driving force G is initially counterbalanced by the increase in crack growth resistance R under rising load, enabling crack growth to be stable [6]. It is well known that the instability condition is reached when:

*Corresponding author: R. Citarella, Tel.: +39-089-964082; fax: +39-089-964037. E-mail-address: rcitarella@unisa.it.

$$G = R \quad \text{and} \quad \frac{dG}{da} = \frac{dR}{da} \quad (3)$$

Usually R is expressed in Stress Intensity Factor (SIF) units, i.e. $K_R = \sqrt{ER}$.

The work on R-curves and their use has been reviewed in [7]. Kraft *et al.* suggested that the R-curve is independent of the initial crack length a_0 ; it is a function of the amount of crack growth only. This implies that failure can be predicted for any initial crack length by a simple construction on the R-curve derived for one value of a_0 [6]. The Rcurve method has been used, for instance, to calculate residual strengths of cracked panels reinforced with stiffeners [8, 9].

2. Problem and 2D-modelling description

The numerical methodology for a Linear Elastic Fracture Analysis, is based on the Dual Boundary Element Method (DBEM) [10], as implemented in the BEASY code [11].

The J-integral technique and the Crack opening Displacement method (COD) are respectively adopted for Stress Intensity Factors (SIF's) evaluation on 2d and 3d numerical models.

The residual strength analysis on the butt-joint is assessed with reference to a pre-cracked specimen, tested by a university laboratory (specimen MSDL3) [12]. The specimen (Fig. 1), which undergoes a slowly increasing load (uniform distribution of tractions t) up to the final failure, has been modelled by a 2D single plate, the influence of the other plate in the joint being modelled by the forces transferred through the pins. The initial cracked configuration is consistent of a central main crack with one cracked hole on each side (Fig. 2).

A constant traction t is imposed on one side of the panel which is constrained in the pin holes against y-translation (Fig. 2) in order to model pin actions, whilst no constraints are present in x-direction in order to allow transversal plate shrinkage. With such constraints, longitudinal plate compliance in the overlapping

area is neglected whilst it is underestimated in transversal x-direction, introducing an element of approximation, that could be circumvented by modelling both plates, still in a 2d analysis but with a more costly analysis and without a relevant overall accuracy improvements in this peculiar application (very long cracks are involved with non negligible elasto-plastic effects). Moreover, due to the two-dimensional hypothesis, the secondary bending [13] is neglected, but this is acceptable because in the area of interest, due to the long cracks, there is a reduced bending stiffness of the plate and consequently a reduced secondary bending influence (as will be shown in the following). The material properties, used for both plate and pin, are: Young modulus $E=72000 \text{ N/mm}^2$ and Poisson ratio $\nu=0.3$.

In the critical cracked area, the pin action modelling has been improved by effectively inserting such pins in the holes and moving the constraints on the pin centre (Fig. 2). In particular, traction and displacements continuity conditions are imposed on 180 degrees (90 for the pin in the main crack) of the pin-hole interface area (the supposed contact area after loading), whilst the remaining part is disconnected by internal spring of negligible stiffness (Fig. 2).

By means of a convergence study, it has been assessed that it is necessary to explicitly model pins just for cracked holes and those nearby, whilst the remaining holes can be simply constrained against y-translation, (Fig. 2). Moreover the convergent mesh was found to be about 1300 quadratic (for both geometric and functional interpolation) elements, with discontinuous elements on the crack sides, semi-discontinuous on the hole boundary at the attachment of the crack and continuous elsewhere.

Gap elements have also been introduced, to better tackle contact conditions but the solution improvement has been judged negligible (less than 2%), except in case of very short cracks emanating from the holes (not relevant in a residual strength analysis), that are more sensitive to pin-hole contact conditions. For this reason, and due to the computational effort of a non-linear analysis, gap elements have no longer been used.

It has been proved that, after link up of cracks between holes, there is no longer a load transfer through the pins in the central part of the main crack (they are generally broken in reality) and that is the reason for they are not modelled with the exception of the extreme ones.

Even in a linear elastic formulation, the SIF's evaluation can be improved by taking into account the elasto-plastic effects, clearly not negligible in a residual strength analysis. This is possible with the Irwin correction, which suggests to prolong the cracks considered of a virtual quantity $r_y = r_p$, where it is possible to assume:

$$r_p = K_{eq}^2 / (S_y^2 * 6.28) \quad (4)$$

as a characteristic dimension of the plastic zone (plastic radius) at the crack tip [14] (S_y is the yield stress).

Two complementary approaches are proposed for failure assessment:

- Plastic collapse prediction, based on Von Mises stress exceeding 385 MPa, the average of yield ($S_y=330$ N/mm²) and rupture stress ($S_u=440$ N/mm²), in large zones of ligament;
- R-curve analysis for stable and unstable crack growth assessment [15].

In the R-curve diagram there are two important points:

1. K_0 is the minimum SIF which gives rise to crack propagation;
2. K_c is the critical stress intensity factor (instability point).

K_c is strongly influenced by the specimen thickness: thinner specimens give higher K_c values and consequently exhibit longer stable crack growth. A sufficiently thick specimen will result in full plane strain and K_c will then be equal to K_0 .

In order to obtain a crack driving energy (or force) curve an iterative process is needed and it is based on the following steps:

- the load is monotonically increased by little steps and for each of them a linear elastic fracture analysis is performed by the DBEM to work out the SIF's;
- at each step the cracks are prolonged by a length da_i which is provided by the R-curve as a function of the SIF's determined at the previous step; moreover, when the plastic effects become significant, cracks are additionally prolonged by a virtual length ξ , in order to provide the Irwin correction for SIF's evaluation. In order to speed up the algorithm, when there is a little crack scenario variation between one load step and the following, SIF's are analytically calculated, supposing a linear variation with load of the SIF's worked out at the previous step;
- for each crack tip, the G curve is drawn and superimposed to the R-curve in order to find out the instability point, as resulting from the conditions (3);
- during the steady crack propagation some cracks will reach a link-up condition with other cracks or holes; such condition is verified when the plastic zone at the crack tip plus the plastic zone of the approaching crack or hole is sufficient to cover the remaining ligament.

The experimental R-curve [12] has the following equation:

$$R=81*da^{0.458} \quad (5)$$

with R expressed in $MPa*mm$ and da in mm .

2.1 Results

The aforementioned procedure gives the following results:

- before the final collapse a steady crack growth of the various cracks results from the R-curve analysis (Table 1);

- the first link-up (Fig. 3) is obtained with a load of 146 MPa (Table 1), that is sufficient to create a plastic zone r_p (from Eq. 4) covering the ligament between the tips 24-25 and between the tips 36-37; the Irwin correction has been adopted for SIF's evaluation because plastic effects become remarkable with such loads;
- increasing gradually the load up to 161 MPa there is a further link-up of tip 23 with the adjacent hole (Table 1); it appears to still exist resistant ligament but just because we have omitted to consider explicitly in Table 1 the hole adjacent plastic zone (the complete ligament yielding is evident from Figs. 4-5);
- after the previous link-up, with the same load $t=161$ MPa there is another link-up of tip 38 with the adjacent hole (Table 1, Fig. 6);
- in this final condition the failure is dictated by plastic collapse, as apparent from Figs.7-8 and Table 1, rather than fracture instability; the experimental collapse load is 167 MPa [12], in good agreement with the numerical one (161 MPa).

In order to assess the level of approximation coming from the two-dimensional hypothesis (plane stress), applied for the residual strength assessment of a butt joint, a 3D model has been also studied.

In particular, a 3D joint modelling is useful for assessing the relevance of the “secondary bending effect” (Fig.9), caused by the offset between the joined plates and the butt strap (which connect them) and clearly neglected in a 2D analysis. Such out of plane bending effect is explicitly modelled in a three-dimensional approach, in order to assess its influence on the variation of SIF's values along the crack front.

3. Butt joint three-dimensional modelling

A 3D BEM modelling of the entire joint is not a viable solution, due to the enormous number of degrees of freedom that would be involved (shell elements are not available in BEASY code), but such limitation can be

circumvented by a sub-region analysis based on a mixed 2D-3D approach. As a matter of fact, at a sufficient distance from the riveted region, the phenomena is essentially two-dimensional with negligible “secondary bending effects”, so that the elastostatic solution from a 2D analysis is judged quite acceptable.

The 3D model is built up by extracting the riveted region from the overall joint 2D model (Fig. 10) and imposing, as boundary conditions along the sub-domains interface, the stresses (σ_{xx} , σ_{yy} , τ_{xy}) coming from the 2D analysis. To this aim a sufficient number of internal points was defined in the 2D BEM model of the joint (Figs. 10-11) and the related stresses (coming from the 2D analysis) imposed on the 3D model as boundary conditions (Fig. 12).

The cracked configuration was approximated as symmetric by applying normal constraints on the lateral surface corresponding to the centre line (Fig. 12). Out of plane stresses are clearly present along the sub-domains interface but they are unknown because not available from the 2D analysis, consequently they were modelled by springs of adequate stiffness on one side, in order to allow a plate movement in the z direction, and zero displacement constraints on the other side, both acting along the borders in the out of plane direction (Fig.12).

Comparative numerical tests showed that it is not necessary to explicitly model the contact conditions by gap elements on the faying surfaces (see also [12]) due to the negligible normal contact stresses between the joined plates (modelling such contact conditions would provide a small difference only on the main crack SIF's). Such simplification drastically reduces the complexity of the non linear analysis, that is still necessary in order to accurately model the contact conditions between the pin and the cracked hole (Fig. 13).

It is interesting to highlight the possibility, given by the BE methodology, of using “discontinuous elements” around the cracked region (Fig. 13): such capability is very useful for refining the mesh only where necessary (high stress gradient regions).

All the pins related to the main crack are supposed broken and consequently not explicitly modelled (Figs. 11-12), whilst the pin in the cracked hole (cracks 1 and 2) is modelled by gap elements; anyway, due to the consistent length of the emanating cracks, comparable to the hole radius, the loss of accuracy related to a completely linear analysis is less than 3%.

The mesh adopted, after a convergence study, is based on 2363 elements, linear and “reduced quadratic” (an 8 node quadrilateral element without the central node). Reduced quadratic elements were applied on the crack surface and nearby the crack front, in order to reproduce the high stress gradients. Continuity pin-hole interface conditions are imposed on all the remaining undamaged holes.

Run times for the non-linear analysis are few hours with a powerful PC.

3.1 Three-dimensional analysis result

The SIF's values along the crack front of the three cracks (Fig. 14), as coming from the 2D and 3D analysis, are illustrated in Fig. 15 with reference to mode I, whilst mode II values are one order of magnitude inferior and mode III values are negligible.

It is interesting to highlight the limited increase of SIF's along the crack front towards the hidden surfaces where the bending stresses add up to the traction stresses, showing a limited influence of the secondary bending effect on very long cracks: this is explained by the local strong reduction in plate bending stiffness due to the weakening effect of the main crack .

The secondary bending effect on the joint deformation, is apparent on the undamaged side from Fig. 16.

4. Conclusions

The 2D procedure for residual strength assessment of a cracked aeronautic butt-joint shows a satisfactory agreement with experimental results, very attractive run times and an easy pre-processing phase.

In this case the failure has been dictated by plastic collapse rather than crack growth instability.

Further investigations with a 3D model of the same joint showed that for residual strength problems (where very long cracks are considered) neglecting the secondary bending effect, as done in the 2D analysis, does not strongly affect the SIF's variation along the crack front of the main crack and adjacent cracks; such SIF's are the highest and consequently the most important in failure assessment.

Anyway, as expected, a non negligible difference exists between the crack front average SIF's values coming from the 3D analysis and the corresponding 2D results (Fig 14).

Our opinion is that for residual strength assessment on aeronautical joints like those considered in this work, when very long cracks are considered, it is possible to assess the validity, as a first approximation, of the 2D analysis results related to the main cracks.

References

1. Standard practice for R-curve determination, ASTM E 561-86, Annual book of ASTM standard, 1990.
2. DeWit R., Fields R.J., Low III S.R., Harne D.E., Foecke T., Fracture Testing of Large Scale Thin Sheet Aluminium Alloy. In: DOT/FAA/AR-95/11 Federal Aviation Administration, 1996.
3. Collins R.A., Residual strength of thin sheets with Multiple Site Damage, Document No. SMAAC-TR-2.3-05-1.2/Bae, December 1998.
4. Broek D., Elementary Engineering Fracture Mechanics, 4th edition, Leyden, Noordhoff, 1974.
5. Feddersen C.E., Evaluation and prediction of residual strength of center cracked tension panels. In: Rosenfield M.S. editor, Damage Tolerance in Aircraft Structures, ASTM STP 486 1971.
6. Kraft J.M., Sullivan A.M. & Boyle R.W., Effect of dimensions on fast fracture instability of notched sheets. In: Proceedings of the Crack Propagation Symposium, Cranfield, 1961.
7. Schwalbe K.H. & Setz W., R-curve and fracture toughness of thin sheet materials, J. Test and Eval. 1981; 9:182-194.

8. Broek D. *et al.*, Fail-safe design procedures. In: Liebowitz H. editor, Fracture Mechanics of Aircraft Structures, AGARDograph, 1974. No. 173, p.120-369.
9. Vlieger H. *et al.*, Built-up structures. In: Liebowitz H. editor, Practical Applications of Fracture Mechanics, AGARDograph, 1980. No. 257, p. 3-1 : 3-113.
10. Portela A. Dual Boundary Element Analysis of Crack Growth. In: C.A. Brebbia and J.J. Connor editors, Topics in Engineering, vol. 14. Southampton: Computational Mechanics Publications, 1990.
11. Beasy Crack Growth Guide Book. Southampton: Computational Mechanics BEASY, 1994.
12. Cattaneo G., Cavallini G., Galatolo R. Testing of "Simple" Specimens, Document No. SMAAC-TR-3.2-07-1.3/AEM, June 1998.
13. Fawaz S.A., Fatigue Crack Growth in Riveted Joints. *Doctoral Thesis*, Delft University Press, The Netherlands, 1997.
14. Broek D., The Effects of Multi-Site-Damage on the Arrest Capability of Aircraft Fuselage Structures, FractuREsearch, TR 9302, June 1993.
15. Apicella A., Citarella R., Esposito R., MSD residual strength assessment for a cracked joint. In: Fracture and Damage Mechanics, Conference proceedings, London, 1999.

Fig. 1. Butt joint analysed (30 rivets per row).

Fig. 2. Close up of the joint cracked area: mesh and boundary conditions for the initial configuration.

Fig.3. Crack scenario after the first link-up between cracks 24-25 and 36-37.

Fig.4. Von Mises stresses on the ligament between tip 23 and the adjacent hole.

Fig.5. Internal points on which Von Mises stresses have been calculated and deformed plot.

Table 1

Fig. 6. Final configuration at the moment of plastic collapse; remote traction applied $t=161$ MPa.

Fig. 7. Von Mises stresses on the right hand side of the main crack (remote traction $t=161$ Mpa).

Fig. 8. Von Mises stresses on the left side of the main crack (remote traction $t=161$ MPa).

Fig. 9. Deformed plot of a lap joint (for the butt joint it is analogous) and through the thickness stress distribution, showing the secondary bending effect.

Fig. 10. Overall two-dimensional joint model and close-up of the cracked area.

Fig. 11. Close up of the riveted region, to be modelled as 3D.

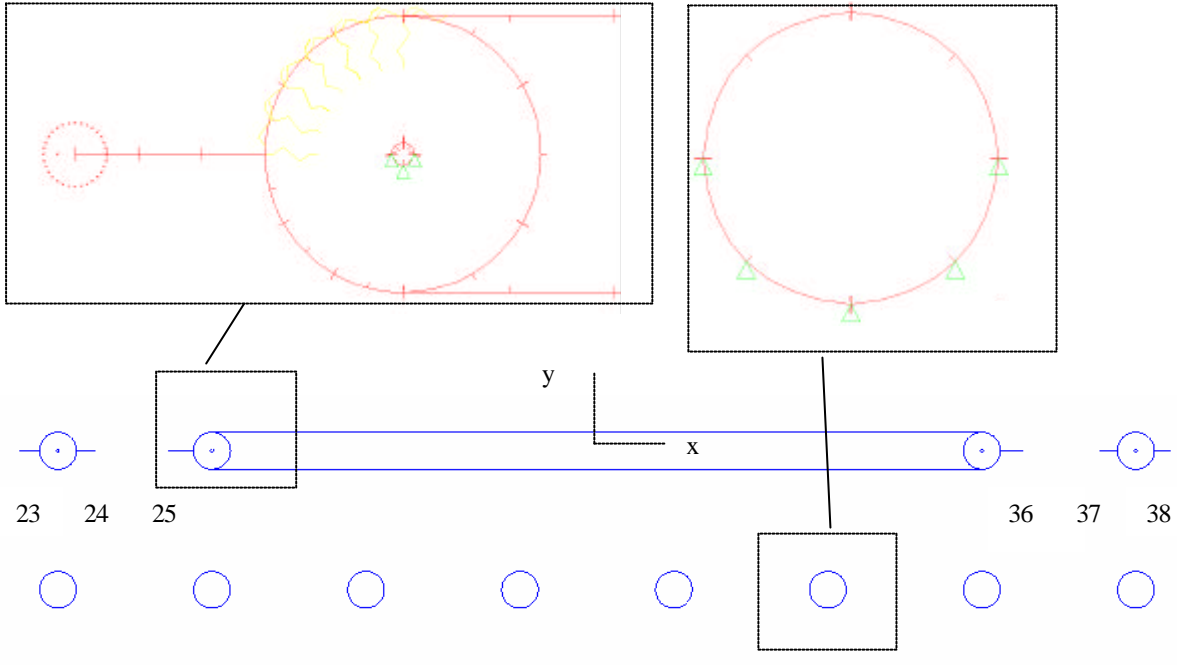
Fig. 12. Butt-joint 3D sub-model: mesh and boundary conditions on a deformed plot.

Fig. 13. Deformed plot of the cracked area and Von Mises stresses.

Fig 14. Cracked area: internal view.

Fig. 15. Mode I SIF's values ($\text{MPa}\cdot\text{mm}^{1/2}$) along the crack front of the three cracks (the hidden surface is at $z=-1.6$ mm), for 3D and 2D model.

Fig. 16. Magnified deformed plot (scale factor 15): it is possible to see the influence of secondary bending on the deformation.

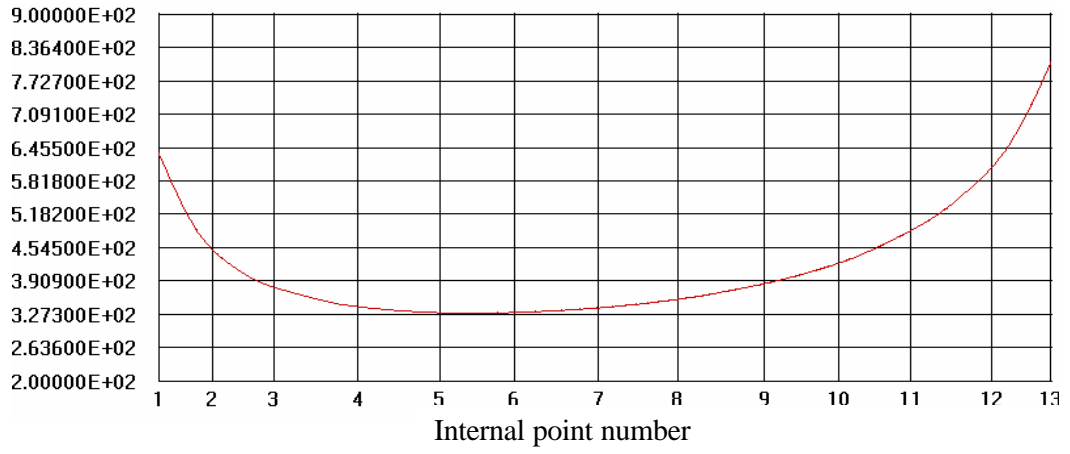


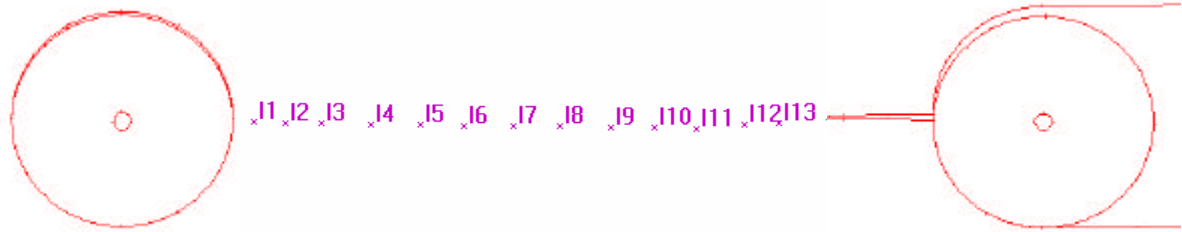


23

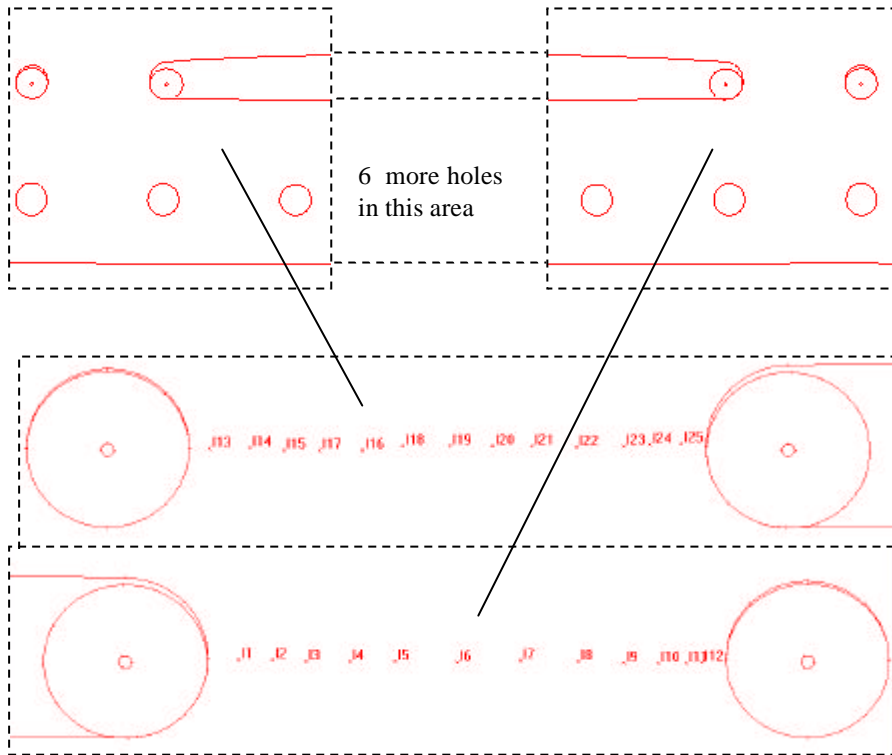
38

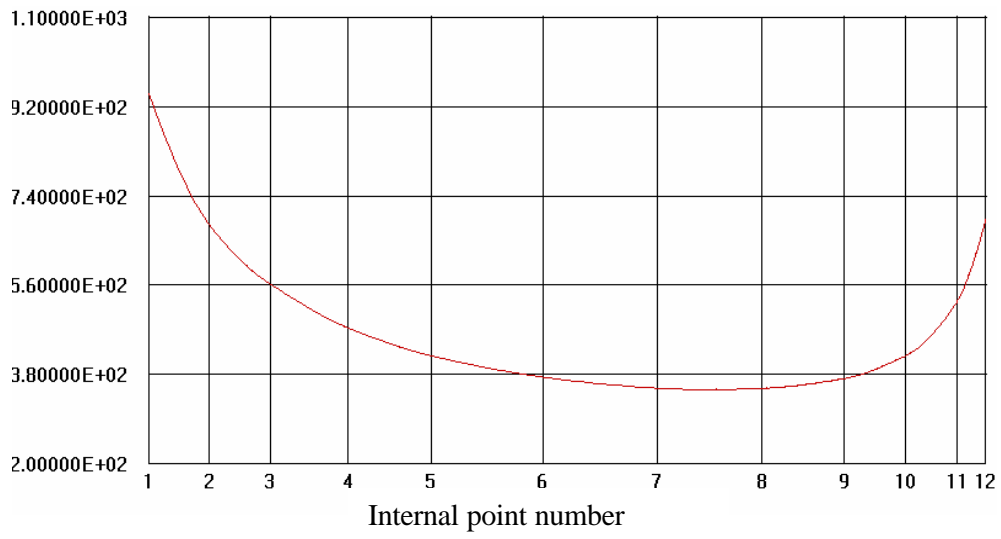


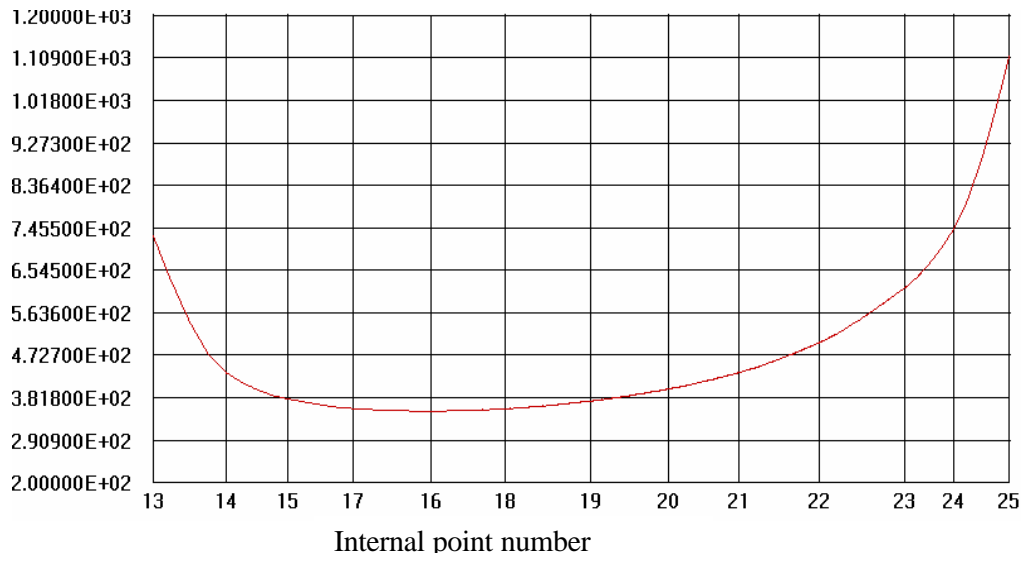


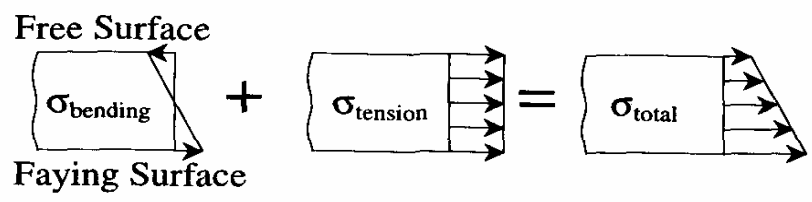
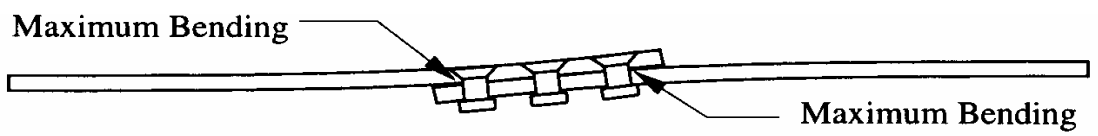


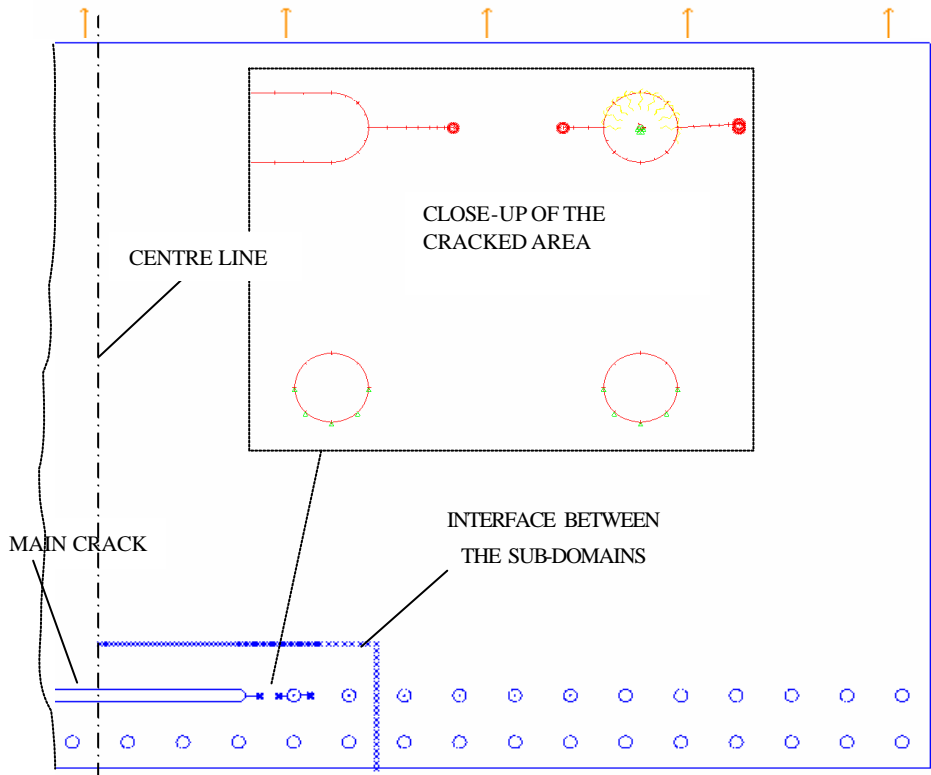
Tip23							
Iter.	σ	$\Delta \sigma$	$a_{in} + da_t + r_y$	K_{eq}	resid. ligam.	da	r_y
	(MPa)	(MPa)	(mm)	(MPa*mm ^{1/2})	(mm)	(mm)	Irwin correc. (mm)
1	136	10	6.79	1114	10.81	0.03	1.79
2	146	10	7.18	1219	10.42	0.05	2.15
3	156	5	11.29	2073	6.31	0.51	6.21
4	161	yielding	12.78	2139	4.82	0.58	6.61
TIP 24							
Iter.	σ	$\Delta \sigma$	$a_{in} + da_t + r_y$	K_{eq}	resid. ligam.	da	r_y
	(MPa)	(MPa)	(mm)	(MPa*mm ^{1/2})	(mm)	(mm)	(Irwin corr.)
1	136	10	7.47	1357	2.73	0.08	2.66
2	146	yielding	8.20	1513	0.90	0.13	3.31
TIP 25							
Iter.	σ	$\Delta \sigma$	$a_{in} + da_t + r_y$	K_{eq}	resid. ligam.	da	r_y
	(MPa)	(MPa)	(mm)	(MPa*mm ^{1/2})	(mm)	(mm)	(Irwin corr.)
1	136	10	9.80	1686	1.07	0.21	4.11
2	146	yielding	10.90	1862	0.90	0.32	5.01
TIP 36							
Iter.	σ	$\Delta \sigma$	$a_{in} + da_t + r_y$	K_{eq}	resid. ligam.	da	r_y
	(MPa)	(MPa)	(mm)	(MPa*mm ^{1/2})	(mm)	(mm)	(Irwin corr.)
1	136	10	9.14	1640	3.72	0.18	3.89
2	146	yielding	10.14	1805	2.07	0.28	4.71
TIP 37							
Iter.	σ	$\Delta \sigma$	$a_{in} + da_t + r_y$	K_{eq}	resid. ligam.	da	r_y
	(MPa)	(MPa)	(mm)	(MPa*mm ^{1/2})	(mm)	(mm)	(Irwin corr.)
1	136	10	7.15	1304	6.51	0.07	2.46
2	146	yielding	7.79	1450	2.07	0.11	3.04
TIP 38							
Iter.	σ	$\Delta \sigma$	$a_{in} + da_t + r_y$	K_{eq}	resid. ligam.	da	r_y
	(MPa)	(MPa)	(mm)	(MPa*mm ^{1/2})	(mm)	(mm)	(Irwin corr.)
1	136	10	6.34	1110	11.26	0.03	1.78
2	146	10	6.73	1215	10.87	0.05	2.13
3	156	5	10.61	2032	6.99	0.46	5.97
4	161	0	11.46	2097	6.14	0.53	6.35
5	161	yielding	14.01	2292	3.59	0.78	7.59











INTERNAL POINTS WHERE TO CALCULATE THE STRESSES FOR THE 3D ANALYSIS BOUNDARY CONDITIONS ASSESSMENT

